NUMERICAL SIMULATIONS OF THE ENERGY-STABLE SCHEME FOR SWIFT-HOHENBERG EQUATION

by

Jun ZHOU*

School of Mathematics and Statistics, Yangtze Normal University, Chongqing 408100, China

A collocation Fourier scheme for Swift-Hohenberg equation based on the convex splitting idea is implemented. To ensure an efficient numerical computation, we propose a general framework with linear iteration algorithm to solve the nonlinear coupled equations which arise with the semi-implicit scheme. Following the contraction mapping theorem, we present a detailed convergence analysis for the linear iteration algorithm. Various numerical simulations, including verification of accuracy, dissipative property of discrete energy and pattern formation, are presented to demonstrate the efficiency and the robustness of proposed method.

Key words: Swift-Hohenberg equation; energy stability; collocation Fourier method; linear iteration

Introduction

The Swift-Hohenberg (SH) equation is an important physical model and can be applied in roll patterns in Rayleigh-Bénard convection in [1], chemical reactions[2], and liquid crystal displays [3,4].

The SH equation is given by the L^2 gradient flow,

$$\frac{\partial u}{\partial t} = -\frac{\delta \mathcal{E}}{\delta u} = -u^3 + \gamma u - \epsilon^2 \Delta u - \delta^2 \Delta^2 u \qquad (1)$$

on$\Omega = [0, L_x] \times [0, L_y]$, and γ, δ^2 and ϵ^2 are positive real constants. Here we only consider the periodic boundary value condition.

Regarding to the numerical consideration, it is well known that the numerical treatment of gradient flow poses certain challenges owing to the physical complexity. Energy stability of the proposed numerical scheme is necessary for SH equation. For example, the linearized schemes are given by Cheng et al. in [5] with three undetermined weights and Backofen *et al.* in [6] with a directly linearized formula$(\phi^{k+1})^3 \approx 3(\phi^k)^2\phi^{k+1} - 2(\phi^k)^3$. More extensive applications of energy-stable or energy conservative method to a wide class of physical models also are available. See the related works for wave equations [7, 8], the phase field crystal (PFC) equation [9] and the Cahn-Hilliard equation [10-12], etc.

In general, for most convex splitting numerical works, a local spatial discretization, such as the finite difference or finite element approximation is often used, because some highly efficient nonlinear (for example, the steepest descent method[13]) solvers can be borrowed readily. But a spatial approximation with a global nature, such as spectral or collocation spectral method for SH

Corresponding author, E-mail: flzjzklm@126.com

equation, is very difficult. The key reason is that, the convex splitting scheme usually treats the nonlinear term implicitly, since the nonlinear part corresponds to the convex part of the Lyapunov energy functional. Whereas, for collocation spectral method, the major advantage is that it is easier to implement, and very efficient due to the fast Fourier transform (FFT). In this paper, a first-order convex splitting scheme, with a collocation Fourier method for the SH equation (1) is proposed. To implement the nonlinear numerical scheme, a linear iteration algorithm is introduced and the corresponding contraction mapping property under a given condition is shown.

The remainder of this paper is organized as follows. In Section 2, we present a semi-implicit scheme for the SH equation (1). A linear iteration algorithm for solving the nonlinear scheme and the corresponding theoretical analysis of the contraction mapping are given in Section 3. Some numerical simulation results are given to demonstrate the convergence order and the discrete energy dissipation law of the proposed numerical scheme in Section 4.

The numerical scheme

Collocation Fourier spectral discretization space

Assumethat $L_x = N_x \cdot h_x,\ L_y = N_y \cdot h_y$ for some mesh sizes $h_x, h_y > 0$ and some positive integers N_x and N_y. For simplicity of presentation, we use a square domain, i.e., $L_x = L_y = 1$, and a uniform mesh size $h_x = h_y = h,\ N_x = N_y = N$. We will always assume that $N = 2K + 1$ is always odd. All the variables are evaluated at the regular numerical grid (x_i, y_j), with $x_i = ih,\ y_j = jh,\ 0 \le i, j \le N$.

For a periodic function f over the given 2D numerical grid, its discrete Fourier expansion is given by

$$f_{i,j} = \sum_{l,m=-K}^{K} \hat{f}_{l,m} \exp(\pi i(lx_i + my_j)) \tag{2}$$

its collocation Fourier spectral approximations to first and second order partial derivatives are givenby

$$(\mathcal{D}_x f)_{i,j} = \sum_{l,m=-K}^{K} (2\pi i l)\, \hat{f}_{l,m} \exp(2\pi i(lx_i + my_j))$$

$$(\mathcal{D}_x^2 f)_{i,j} = \sum_{l,m=-K}^{K} (-4\pi^2 l^2)\, \hat{f}_{l,m} \exp(2\pi i(lx_i + my_j)) \tag{3}$$

and the corresponding collocation spectral differentiations in the y direction can be defined in the same way.

We introduce the ℓ^∞ and $\ell^p, \ell \le p < \infty$ norms for a grid function,

$$\| f \|_\infty := \max_{0 \le i,j \le N-1} | f_{i,j} |, \qquad \| f \|_p := (h^2 \sum_{i,j=0}^{N-1} | f_{i,j} |^p)^{1/p} \tag{4}$$

The following lemma will play important role in the contraction mapping analysis for our algorithm.

Suppose$\gamma_1, \gamma_2 > 0$. For any periodic grid function f, we have,

$$2C_0\alpha\| f \|_4^2 \le \gamma_1 \| f \|_2^2 + \gamma_2 \| \nabla_N f \|_2^2 \tag{5}$$

where $\alpha = -2\gamma_2 + 2\sqrt{\gamma_2(\gamma_1 + \gamma_2)}$.

Proof. For the proof of (5), a discrete version of Sobolev embedding from H_h^2 (the discrete case of H^2 space) into ℓ^4, we have to utilize the grid function f with its discrete Fourier expansion defined as (2). An application of discrete Parseval equality gives

$$\| f \|_2^2 = \sum_{l,m=-K}^{K} | \hat{f}_{l,m} |^2, \quad \| \nabla_N f \|_2^2 = \sum_{l,m=-K}^{K} \lambda_{l,m} | f_{l,m} |^2, \quad \| \Delta_N f \|_2^2 = \sum_{l,m=-K}^{K} \lambda_{l,m}^2 | f_{l,m} |^2 \tag{6}$$

with $\lambda_{l,m} = 4\pi^2(l^2 + m^2)$. Then, letting

$$\gamma_1 = \alpha + \beta, \ \alpha > 0, \beta > 0 \tag{7}$$

we have

$$\begin{aligned} \gamma_1 \| f \|_2^2 + \gamma_2 \| \Delta_N f \|_2^2 &= \alpha \| f \|_2^2 + \sum_{l,m=-K}^{K} (\beta + \gamma_2 \lambda_{l,m}^2) | \hat{f}_{l,m} |^2 \\ &\geq \alpha \| f \|_2^2 + 2\sqrt{\beta\gamma_2} \sum_{l,m=-K}^{K} \lambda_{l,m} | \hat{f}_{l,m} |^2 = \alpha \| f \|_2^2 + 2\sqrt{\beta\gamma_2} \| \nabla_N f \|_2^2 \end{aligned} \tag{8}$$

Next, we choose values of α and β with $\alpha = 2\sqrt{\beta\gamma_2}$. It follows from (8) that

$$\alpha = -2\gamma_2 + 2\sqrt{\gamma_2(\gamma_1 + \gamma_2)} \quad \beta = \gamma_1 + 2\gamma_2 - 2\sqrt{\gamma_2(\gamma_1 + \gamma_2)} \tag{9}$$

Therefore, from (9), we get

$$\gamma_1 \| f \|_2^2 + \gamma_2 \| \Delta_N f \|_2^2 \geq \alpha \| f \|_2^2 + \alpha \| \nabla_N f \|_2^2 = \alpha \| f \|_{H_h^1}^2 \geq C_0 \alpha \| f \|_4^2 \tag{10}$$

in which a discrete Sobolev embedding from H_h^1 to ℓ^4 is used. This completes the proof.

Semi-implicit numerical scheme

We propose the following fully discrete first-order (in time) Fourier collocation spectral scheme for SH equation (1),

$$\frac{u^{n+1} - u^n}{\Delta t} = -(u^{n+1})^3 + \gamma u^n - \epsilon^2 \Delta_N u^n - \delta^2 \Delta_N^2 u^{n+1} \tag{11}$$

where Δt is the discrete time step and u^n denotes the time-discrete approximation of $u(\cdot, n\Delta t)$, $n = 0,1,\cdots, M = [\frac{T}{\Delta t}]$ and T is a given final time.

Lemma 2. Assume that u^n is the numerical solution of (11). Then, the following estimates are valid:

$$\| u^n \|_4 \leq C_1, \quad \| u^n \|_2 \leq C_2, \quad \| \Delta_N u^n \|_2 \leq C_3 \qquad \| u^n \|_\infty \leq C_4 \tag{12}$$

for $n = 1,2,\cdots, M$.

Linear iteration algorithm

In this section, we mainly discuss an efficient algorithm for solving (11). Firstly, we note that the scheme (11) can be reformulated as a closed equation for u^{n+1}:

$$\left(\frac{1}{\Delta t} + \delta^2 \Delta_N^2 + \epsilon^2 \Delta_N\right) u^{n+1} = \frac{1}{\Delta t} u^n + \gamma u^n - (u^{n+1})^3 \tag{13}$$

or, equivalently,

$$\left(\mathcal{I} + t\delta^2 \Delta_N^2 + t\epsilon^2 \Delta_N\right) u^{n+1} = t\gamma u^n - t(u^{n+1})^3 + u^n \tag{14}$$

where $\mathcal{I}$ denotes the identity operator. Also, define a linear operator $\mathcal{A}$ and the value f_n at the n-th level,

$$\mathcal{A} := \mathcal{I} + t\delta^2 \Delta_N^2 + t\epsilon^2 \Delta_N, \quad f_n = t\gamma u^n - t(u^{n+1})^3 + u^n \tag{15}$$

Then, (14) can be simplified as follows,

$$\mathcal{A}u^{n+1} = f_n - \Delta t(u^{n+1})^3 \tag{16}$$

Obviously, the nonlinear part in this equation is treated implicitly. To overcome the difficulty associated with the implicit treatment of the nonlinear term, a linear solver is necessary, and we propose the following linear iteration algorithm:

$$\mathcal{A}u^{n+1,(k+1)} = f_n - \Delta t(u^{n+1,(k)})^3 \tag{17}$$

in which $u^{n+1,(k)}$ corresponds to the numerical solution at the k-th iteration.

The following theorem gives an affirmative answer for the convergence of such an iteration algorithm.

Theorem 1. The linear iteration (17) is a contraction mapping in the discrete $\|\cdot\|_4$ norm, provided that

$$\Delta t < \frac{C_0^2\delta^2}{5C_1^2(5C_1^2 + 2C_0\delta^2)} \tag{18}$$

with the positive constants C_0, C_1 which are given in (5) and (12), respectively.

Proof. Let u^{n+1} be the unique periodic solution to (14) and define the iteration error at each stage via

$$e^k := u^{n+1,(k)} - u^{n+1} \tag{19}$$

Subtracting (17) from (16) yields the following discrete equation,

$$\mathcal{A}e^{k+1} = -\Delta t((u^{n+1,(k)})^3 - (u^{n+1})^3) \tag{20}$$

Taking a discrete inner product of (20) with e^{k+1}, and using integration by parts leads to

$$\begin{aligned} <\mathcal{A}e^{k+1}, e^{k+1}> &= <e^{k+1}, e^{k+1}> + \Delta t\delta^2 <\Delta_N e^{k+1}, \Delta_N e^{k+1}> = \|e^{k+1}\|_2^2 + \Delta t\delta^2\|\Delta_N e^{k+1}\|_2^2 \\ &= -\Delta t(<(u^{n+1,(k)})^2 + u^{n+1,(k)}u^{n+1} + (u^{n+1})^2, e^k e^{k+1}>) \le \Delta t(|u^{n+1,(k)}\|_4^2 + \|u^{n+1}\|_4^2)\|e^k\|_4 \cdot \|e^{k+1}\|_4 \end{aligned} \tag{21}$$

in which a discrete Hölder inequality was applied at the last step. To proceed the nonlinear analysis, we use the induction method to handle the bound of error function e^k. In general, we choose $u^{n+1,(0)} = u^n$ as the initial value. By the preliminary bound (12) in Lemma 2, we can get an estimate for e^0 in the $\|\cdot\|_4$ norm,

$$\|e^0\|_4 = \|u^n - u^{n+1}\|_4 \le \|u^n\|_4 + \|u^{n+1}\|_4 \le 2C_1 \tag{22}$$

and make the following the inductive assumption at the iteration stage k,

$$\|e^k\|_4 \le 2C_1 \tag{23}$$

With this assumption, a bound of $u^{n+1,(k)}$ in the $\|\cdot\|_4$ norm is derived as follows,

$$\|u^{n+1,(k)}\|_4 \le \|e^k + u^{n+1}\|_4 \le \|e^k\|_4 + \|u^{n+1}\|_4 \le 3C_1 \tag{24}$$

Going back to (21), we consider the term $\|e^{k+1}\|_2^2 + \Delta t\delta^2\|\Delta_N e^{k+1}\|_2^2$. According to Lemma 1, taking $\gamma_1 = 1$ and $\gamma_2 = \Delta t\delta^2$, we have,

$$\|e^{k+1}\|_2^2 + \Delta t\delta^2\|\Delta_N e^{k+1}\|_2^2 \ge (C_0 - \Delta t\delta^2 + 2\sqrt{(\Delta t\delta^2 + 1)\Delta t\delta^2})\|e^{k+1}\|_4^2 \tag{25}$$

which indicates

$$2C_0(1 - \Delta t\delta^2 + \sqrt{(\Delta t\delta^2 + 1)\Delta t\delta^2})\|e^{k+1}\|_4^2 \le \Delta t(\|u^{n+1,(k)}\|_4^2 + \|u^{n+1}\|_4^2)\|e^k\|_4 \cdot \|e^{k+1}\|_4 \tag{26}$$

Hence, it follows from (26) that

$$C_0(1 - \Delta t\delta^2 + \sqrt{(\Delta t\delta^2 + 1)\Delta t\delta^2})\|e^{k+1}\|_4 \le C_1^2\Delta t\|e^k\|_4 \tag{27}$$

and we arrive at the estimate

$$\| e^{k+1} \|_4 \leq \frac{5C_1^2 \Delta t}{C_0(\sqrt{\Delta t\delta^2(\Delta t\delta^2+1)} - \Delta t\delta^2)} \| e^k \|_4 \tag{28}$$

As a result, a contraction is assured under the condition that

$$\frac{5C_1^2 \Delta t}{C_0(\sqrt{\Delta t\delta^2(\Delta t\delta^2+1)} - \Delta t\delta^2)} < 1 \tag{29}$$

that is,

$$\Delta t < \frac{C_0^2 \delta^2}{5C_1^2(5C_1^2 + 2C_0\delta^2)}. \tag{30}$$

Clearly, we are justified in our a priori assumption (23), since

$$\| e^{k+1} \|_4 < \| e^k \|_4 \leq 2C_1, \tag{31}$$

provided that condition (31) is enforced, which completes the proof of Theorem 1.

Numerical experiments

In this section, we present some numerical experiments to verify the theoretical results obtained in the previous sections, particularly the accuracy test, the energy stability and the pattern formation.

Accuracy test

An example provides the numerical evidence for our numerical scheme being first-order accurate in time and spectral accurate in space. The setup of this accuracy test is based on that presented in [11, 14]. We solve the one-dimensional Swift-Hohenberg equation on the domain $\Omega = [0, 32]$. The initial condition is defined as:

$$u(x) = 0.07 - 0.02\cos(\frac{2\pi(x-12)}{32}) + 0.0171\cos^2(\frac{2\pi(x+10)}{32}) - 0.0085\sin^2(\frac{4\pi x}{32}) \tag{32}$$

For exploring the temporal accuracy in time, we fix spatial resolution as $N = 2048$ so that the numerical error is dominated mainly by the temporal ones. We computed a reference solution at time $T = 1$ using a time step $\Delta t = 1/2^{11}$ and assume that this space time discretization is fine enough as to suppose that the reference solution is exact. With a sequence of time step sizes $\Delta t = 0.1, 0.005, 0.025, 0.0125$ and 0.00625, we also compute the numerical errors at $T = 1$ for the parameter group (I): $\gamma = 0.001, \varepsilon^2 = 1, \delta^2 = 1$ and the parameter group (II): $\gamma = 0.025, \varepsilon^2 = 1, \delta^2 = 10$, respectively. The results are presented in Tab. 1 in which a first-order in time accuracy is shown clearly.

Table 1. $\| \cdot \|_2$ errors and convergence orders of the numerical solution at $T = 1$ for different parameter group $\gamma, \varepsilon^2, \delta^2$.

Δt	$\gamma = 0.001, \varepsilon^2 = 1, \delta^2 = 1$	order	$\gamma = 0.025, \varepsilon^2 = 1, \delta^2 = 10$	order
0.1	6.7072556e-6	-	1.3791082e-4	-
0.05	3.3186000e-6	1.015147	6.8618141e-5	1.007073
0.025	1.6374393e-6	1.019133	3.3978888e-5	1.013951
0.0125	8.0141592e-7	1.030818	1.6648254e-5	1.029267
0.00625	3.8417922e-7	1.060771	7.9846732e-6	1.060065

To demonstrate the accuracy in space, we take $\Delta t = 10^{-4}$ so that the temporal numerical error is negligible. Also, we computed a reference solution at time $T = 5$ with $N = 2048$ and assume that this space time discretization is fine enough as to suppose that the reference solution is exact. With grid sizes $N = 8,16,32,64,128$, we solve (11) up to for two different parameter groups given in above subsection, respectively. The discrete norm $\|\cdot\|_2$ of numerical errors at $T = 5$ is given in Tab. 2, which shows the spatial spectral accuracy is verified. Noting that when N increases from 64 to 128, there have so little difference between errors. The main reason is that the value of N is so large that the numerical errors are dominated by the temporal discretization.

Tab. 2 $\|\cdot\|_2$ errors of spectral accuracy for the numerical solution at $T = 5$

Δt	$\gamma = 0.001, \varepsilon^2 = 1, \delta^2 = 1$	$\gamma = 0.025, \varepsilon^2 = 1, \delta^2 = 10$
8	9.21122e-05	1.246072e-06
16	1.37439e-06	1.103986e-12
32	2.67306e-13	2.376737e-14
64	5.71089e-14	3.670676e-14
128	7.14353e-14	4.489314e-14

In this subsection, we present some numerical tests to support the theoretical analysis for the proposed linear iteration algorithm (14). We fix $\gamma = 1, \varepsilon^2 = 1, N = 256$ and $\Delta t = 0.01$. Different values of the coefficient δ^2 and the final time are used to compare the times for the linear iteration. By setting 10^{-9} as the tolerance of iteration error, we present the detailed results in Tab. 3 From Tab. 3, it is clear that the linear iteration error reaches a saturation after certain iteration stages. We observe that the time for the linear iteration increases with a decreasing value of δ^2, which in turn implies that numerical implementation of the linear iteration algorithm (14) becomes more challenging with a smaller diffusion coefficient δ^2. This result matches with our theoretical analysis in the proof of Theorem 1.

Table 3. Iterations of the propose algorithm at different final time T with different δ^2.

δ^2	$T = 4$	$T = 5$	$T = 6$	$T = 7$	$T = 8$	$T = 9$	$T = 10$
1	6	5	5	4	4	3	3
0.1	7	8	8	8	8	8	8
0.01	28	25	25	24	24	24	23

Pattern formation

Localized structures, which can be described by real order parameter equations in the form of Swift-Hohenberg type of models, remain of great interest in the pattern-formation community. In fact, Many recent experimental and theoretical studies have focused exclusively on localized pattern formation[15]. From SH equation (1), one expects to observe the single stripe becomes unstable by the emergence of undulations.

Here the parameters are $\gamma = 1, \varepsilon^2 = 2, \delta^2 = 1$. Take $\Omega = [0, 40]^2$ and fix the spatial resolution as $N = 512$ and the time step as $\Delta t = 0.1$. The initial condition is a constant state $u = -1$ in which we embed a curvy vertical stripe with the phase variable taking the value $u = 1$. The initial pattern evolves developing horizontal fingers that might bifurcate (see Fig.1).

The right part of Fig. 1 illustrates the manifestation of this undulations under the consideration of an infinitely long rod-like structure, to avoid border effects. Later, this undulated

stripe is replaced by the emergence of facets that form a zigzag structure. However, the higher nonlinear terms control the evolution of the single stripe, then the dynamics of initial zigzag is replaced by the growth of undulations without saturation as it is depicted in Fig. 2. The numerical results are consistent with the experiments on this topic in [14].

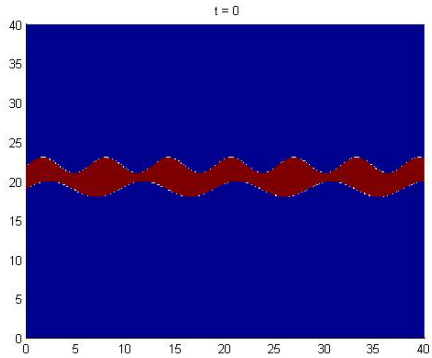

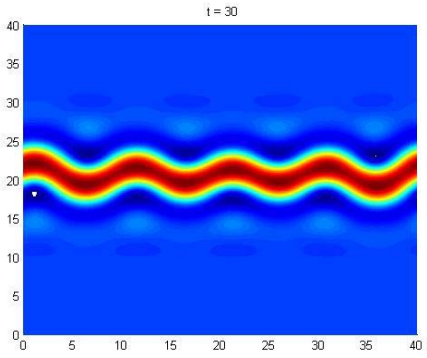

Fig. 1: Initial status of u(x, y) at t = 0. Right: Numerical solution of u at T = 30

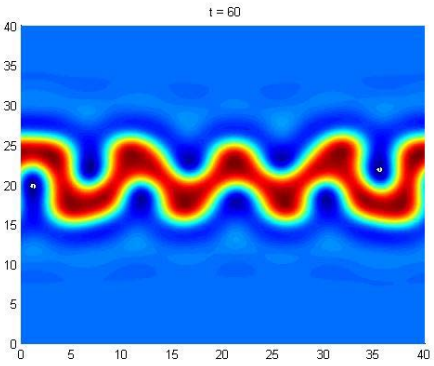

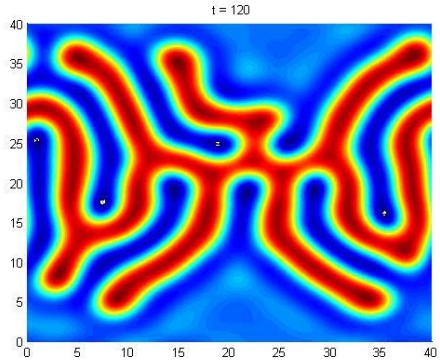

Fig. 2: Initial status of u(x, y) at T = 60. Right: Numerical solution of u at T = 120.

References

[1] Swift, J., Hohenberg,P. C., Hydrodynamic fluctuations at the convective instability, *Phys. Rev. A*,15(1977), 1, pp. 319-328

[2] Vanag,V. K., Epstein,I. R., Stationary and oscillatory localized patterns, and subcritical bifurcations, *Phys. Rev. Lett.*, 92(2004), 12, pp. 1-4

[3] Oswald, P., *et al*., Static and dynamic properties of cholesteric fingers in electric field, *Physics Reports*, 337(2000), 1, pp. 67-96

[4] Ribiere, P., Oswald, P., Nucleation and growth of cholesteric fingers under electric field, *Journal De Physique*, 51(1990), 16, pp.1703-1720

[5] Cheng, M., Warren,J. A., An efficient algorithm for solving the phase field crystal model, *J. Comput. Phys.*, 227(2008), 12, pp. 6241-6248

[6] Backofen, R., *et al*., Nucleation and growth by a phase field crystal (PFC) model, *Phil. Mag. Lett.*, 87(2007), 11, pp. 813-820

[7] Cheng, K., *et al*., A Fourier pseudospectral method for the “good” Boussinesq equation with second-order temporal accuracy, *Numer. Meth. Partial Diff. Eq.*, 31(2015), 1, pp. 202-224

[8] Kang, X., *et al*., An efficient finite difference scheme for the 2D sine-Gordon equation, *J. Nonlinear Sci. Appl.*,10 (2017), 1, pp. 2998-3012

[9] Baskaran, A., *et al.*, Energy stable and efficient finite difference nonlinear multigrid schemes for the modified phase field crystal equation, *J. Comput. Phys.*, 250(2013), 10, pp. 270-292
[10] Cheng, K., *et al.*, A second-order, weakly energy-stable pseudo-spectral scheme for the Cahn-Hilliard equation and its solution by the homogeneous linear iteration method, *J. Sci. Comput.*, 69(2016), 3, pp. 1083-1114
[11] Cheng, K., *et al*., An energy stable fourth order finite difference scheme for the Cahn-Hilliard equation, *J. Comput. Appl. Math*.,1 (2019), 5, pp. 1-22.
[12] Xue, Y., *et al.*,Evaluation of the Non-Darcy Effect of Water Inrush from Karst Collapse Columns by Means of a Nonlinear Flow Model, *Water*,10 (2018), 9, pp. 1234
[13] Feng, W., *et al*., Preconditioned steepest descent methods for some nonlinear elliptic equations involving p-Laplacian terms, *J. Comput. Phys.*, 334(2016), 1, pp. 45-67
[14] Gomez, H., NogueiraX., A new space-time discretization for the Swift-Hohenberg equation that strictly respects the Lyapunov functional, *Commun. Nonlinear Sci. Numer. Simulat.*,17(2012), 12, pp. 4930-4946
[15] Lloyd, D., Sandstede B., Localized radial solutions of the Swift-Hohenberg equation, *Nonlinearity*, 22(2009), 2, pp. 485-524

Paper submitted: May 15, 2018
Paper revised: September 20, 2018
Paper accepted: November 15, 2018